Spectroscopic Properties of Porphyrin-Like Photosensitizers: Insights from Theory

Laurence Petit,[†,‡] Angelo Quartarolo,[†] Carlo Adamo,*[,‡] and Nino Russo[†]

Dipartimento di Chimica and Centro di Calcolo ad Alte Prestazioni per Elaborazioni Parallele e Distribuite Centro d'Eccellenza MURST−Università della Calabria, I-87030 Arcavacata di Rende, Italy, and Laboratoire d'Électrochimie et Chimie Analytique, CNRS UMR-7575, École Nationale Supérieure de Chimie de Paris, 11 rue P. et M. Curie, F-75231 Paris Cedex 05, France

Received: September 5, 2005; In Final Form: November 21, 2005

Electronic absorption spectra of six porphyrin-like photosensitizers, porphyrin, chlorin, bacteriochlorin, pheophytin a, porphyrazin, and texaphyrin, have been calculated within the time-dependent DFT framework (TDDFT) in conjunction with the PBE0 hybrid functional. Energetic and orbital aspects are discussed by comparing systems together so as to assess the best molecules for photodynamic therapy applications. Excitation energies and oscillator strengths are found to be in good agreement with both experimental data and previous theoretical works. In particular, whereas significant discrepancies (0.3 eV) appear for Qx bands, results become more reliable as wavelengths decrease. To elucidate the effect of the local environment, we have taken into account solvation either with explicit water molecules interacting via hydrogen bonds with the system or with a continuum model (C-PCM). The supramolecular approach does not affect spectra, while using C-PCM improves Qx and B band values and strengthens intensities significantly. In both gaseous and aqueous phases, texaphyrin, pheophytin a, and bacteriochlorin Qx bands are found in the 600−800 nm range as expected by experimental works. These data are particularly interesting in the perspective of systematic studies of other photosensitizers and should make experimentalists' works easier.

1. Introduction

Porphyrins and their derivatives are commonly found in nature, and they play very important roles in various biological processes.[1−3] For instance, the heme involved in oxygen transport and storage is based on the complexation of iron by a porphyrin ring. Recently, there has been an increasing interest in the synthesis and characterization of porphyrin-like compounds (e.g., porphyrin, chlorin, bacteriochlorin, porphyrazine, pheophytin, and texaphyrin) due to their use in photodynamic therapy (PDT).[4−6] The basic principle[1] is to inject into the blood a photosensitizing agent that is going to gather into cells. This photosensitizer can be activated under irradiation, and the energy is then transferred to nearby molecules via a radiationless transition. In particular, triplet molecular oxygen ($^3O_2$) can be excited into the singlet state that is cytotoxic and can then destroy possible cancerous cells. The required excitation energy is quite low, about 1 eV (around 1300 nm), and can be easily obtained through several photosensitizers. Within this perspective, numerous experimental works have been devoted to the synthesis of new photosensitizers designed for their absorption at high wavelengths, some of them being currently used for clinical applications.[5,6]

At the same time, tetrapyrroles have been the subject of detailed theoretical studies with the aim to reproduce and rationalize their peculiar electronic characteristics.[7−27] The first theoretical studies are dated back to the late 1940s by Kuhn[21] and Simpson.[22] Semiempirical approaches were then attempted,[23−25] and the progressive development of quantum methods nowadays enables obtaining of very good agreement with experimental data for these kinds of systems. Among these techniques, the time-dependent extension of the density functional theory TDDFT[28] has proved its efficiency in the evaluation of electronic spectra for a wide range of compounds, including porphine rings.[7,18,20] Calculations of vertical excitation energies and oscillator strengths are indeed less cumbersome than highly correlated ab initio methods and provide comparable accuracy.[29] Such advantages are particularly interesting when dealing with large molecules such as tetrapyrroles. Moreover, the large number of possible candidate photosensitizers[4] makes it necessary for experimentalists to have a routine methodology to select only the most promising molecules.

In this paper, we have undertaken the systematic study of the excited states of six porphyrin-type systems by using the TDDFT approach, i.e., free base porphyrin (FBP), free base chlorine (FBC, also called dihydroporphyrin), free base bacteriochlorin (FBBC, also called tetrahydroporphyrin), pheophytin a (Pheo a), porphyrazine (Pz, also called tetraazaporphyrin) and texaphyrin (Tex1 and Tex2). Their structures are sketched in Figure 1. These systems should be sufficiently stable in aqueous solution and preserve their spectroscopic properties in biological media. Consequently, any realistic theoretical analysis should be carried out by taking into account the interactions with the local environment (i.e., solvent) in order to give meaningful insights on the elementary excitation mechanisms. Solvent effects on electronic properties have thus been taken into account either by considering a few explicit water molecules (supramolecular approach) around the macrocycle, or implicitly by using a continuum solvent model. The first approach is mandatory because protic solvents (like water) could be involved in H-bonding with the solute, while the reaction field of the bulk solvent could significantly modulate the spectral properties of the systems.[30,31]

* Corresponding author. E-mail: carlo-adamo@enscp.fr.
† Università della Calabria.
‡ ENSCP.

10.1021/jp055016w CCC: $33.50 © 2006 American Chemical Society
Published on Web 01/12/2006

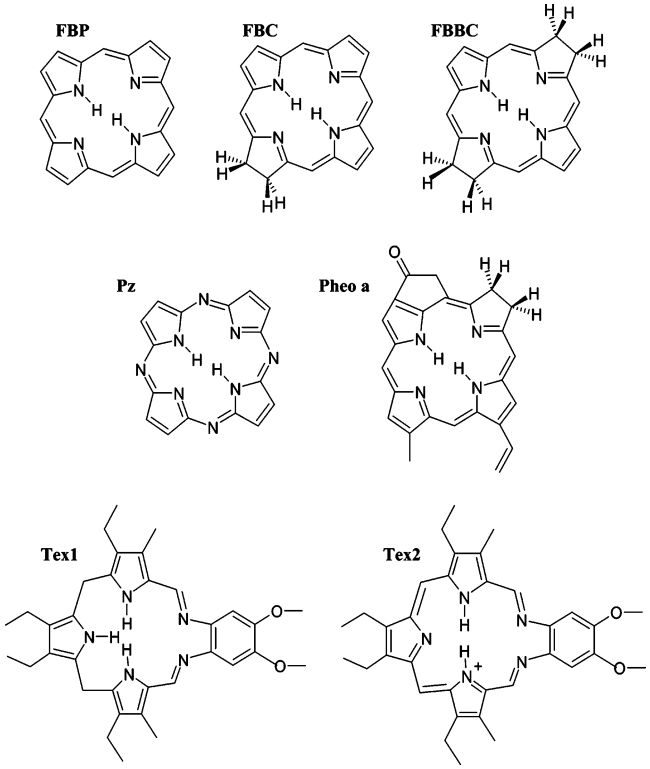

Figure 1. Sketches of the considered molecules: FBP, FBC, FBBC, Pz, Pheo a, Tex1, and Tex2.

2. Computational Details

DFT calculations were carried out with the Gaussian 03 package[32] with the hybrid functional PBE0.[33] This functional is based on the generalized gradient functional PBE (Perdew−Burke−Erzenrhof)[34] with 25% of exact exchange.

Structures have been fully optimized both in vacuo and with explicit water molecules by using the 6-31G(d) basis set[35] and the correct symmetry group, i.e., D_{2h} for FBP, FBBC, and Pz, C_{2v} for FBC, C_2 for Tex2, C_s for Pheo a, and without symmetry for Tex1. These symmetries were lowered for calculations with explicit water molecules. Notice that, as reported by Hasegawa and co-workers,[36] we have replaced some substituents of Pheo a by hydrogens.

Absorption spectra were computed as vertical excitations from the minima of the ground-state structures by using the TDDFT approach, as implemented in the Gaussian code[37] and the 6-31+G(d) basis set.[35] On the basis of our previous experience, we expect that this level of theory (PBE0/6-31+G(d)) will provide an error not larger than 0.4 eV on the systems investigated[20,29]

Solvent effects were evaluated by using the conductor-like approach within the framework of the polarizable continuum model (C-PCM).[38,39] This approach provides results very close to those obtained by the original dielectric model for high-dielectric-constant solvents, but it is less prone to numerical errors arising from the small part of the solute electron cloud lying outside the cavity (escaped charge effects). Solvent shifts of excitation bands were evaluated by a recent nonequilibrium implementation[40] of the polarizable continuum model by using gas-phase structures.

3. Results and Discussion

3.1. Excited States in a Vacuum. Because of their highly conjugated ring, porphyrin-like systems show intense absorption around 400 nm, the so-called Soret or B bands, followed by weaker satellites between 500 and 800 nm, known as Q bands. Their spectra can be roughly rationalized in terms of the four-orbital Gouterman's model, where the principal excitations involve the two highest occupied molecular orbitals (HOMO and next-HOMO) and the two lowest unoccupied molecular orbitals (LUMO and next-LUMO).[41] The substitution or the modification of the porphine ring can affect these levels in different ways. Among these changes, the hydrogenation of outer carbon double bonds, resulting in FBC and FBBC (Figure 1), has a great effect on the absorption spectrum. The direct consequence is a decrease in the number of π electrons involved in the aromatic system, with 22, 20, and 18 π electrons for FBP, FBC, and FBBC, respectively. The related effects on the spectra are clearly evidenced by the results reported in Table 1 and in Figure 2. Qx bands are indeed red-shifted as one goes from FBP (532 nm) to FBC (544 nm) and FBBC (590 nm). These values are in good agreement with experimental data,[42−44] with a mean absolute error of 0.2 eV. Similar discrepancies were reported by previous TDDFT calculations.[7,12] A slightly larger variation (0.4 eV) is nevertheless found for FBBC, whose experimental reference does not correspond to the free base bacteriochlorin but rather to the larger bacteriopheophorbide. Some comments about TDDFT failures on the zincbacteriochlorin−chorin complex have been proposed by Dreuw and co-workers, but they are related to intermolecular excitations between two different subunits.[45]

Along this series, the Qx band is mainly composed of the HOMO → LUMO transition and in a smaller amount of the next-HOMO → next-LUMO. The Qy counterpart equally corresponds to next-HOMO → LUMO and HOMO → next-LUMO excitations. These orbitals are depicted in Figure 3, and their energies are plotted in Figure 4. An exception is represented by FBP, whose frontier orbitals are quasidegenerate (Figure 4). Therefore, the transition assignment can change from one calculation to another one; there is indeed an inversion in Q band assignments between attributions in vacuo and in aqueous solution (see Table 1).

For FBC and FBBC, the reduction of pyrrole rings results in a conjugation breakdown. Figure 3 indeed shows that HOMO and next-LUMO energies increase because there is some amplitude on reduced pyrroles on these levels (see Figure 4). In contrast, there is no participation on next-HOMO and LUMO, so their energies are quite constant whatever the molecule is. The relaxation of degeneracy of HOMO and next-LUMO makes the HOMO/LUMO difference smaller, whereas the next-HOMO/next-LUMO gap is strengthened. Wavelengths of the Qx bands are, therefore, enhanced, and the corresponding oscillator strengths are also affected. As proposed by Weiss,[46] FBP is perfectly symmetric, so transition moments of the first two excitations are quite the same but in opposite directions. They cancel each other, and the intensity of the excitation is very low (forbidden in our work). In contrast, the symmetry variation in FBC and FBBC induces a partial cancellation of transition moments, and the oscillator strength is consequently raised ($f_{FBC} = 0.098$; $f_{FBBC} = 0.243$).

The same trend is observed for Qy bands ($f_{FBP} = 0.000$; $f_{FBC} = 0.001$; $f_{FBBC} = 0.048$), but contrary to the Qx ones, they are slightly blue-shifted from FBP (498 nm) to FBC (491 nm) and FBBC (483 nm). Next-HOMO → LUMO and HOMO → next-LUMO transitions are indeed affected in a smaller amount, as one can see in Table 1. Note that the agreement with experimental data is better than for Qx bands, with errors of 0.07 eV for FBP, 0.23 eV for FBC, and 0.27 eV for FBBC.

TABLE 1: Excitation Energies (eV and nm), Oscillators Strengths, Configurations, and Experimental Data for FBP, FBC, FBBC, and Pz[a]

	vacuum			solution (water PCM)			expt		
state	excitation energy	f	main configuration	excitation energy	f	main configuration	excitation energy	f	assignment
				FBP					
B1u	2.33 (532.10)	0.000	45%(1−0) + 55%(0−1)	2.36 (526.24)	0.0003	45% (1−1) + 55% (0−0)	1.98[b]	0.01	Qx
B2u	2.49 (498.41)	0.000	48% (1−1) + 52% (0−0)	2.50 (496.60)	0.0001	51% (0−1) + 49% (1−0)	2.42	0.06	Qy
B1u	3.43 (361.28)	0.613	40% (3−1) + 38% (1−0) + 22% (0−1)	3.34 (371.19)	1.147	17% (3−0) + 51% (1−1) + 32% (0−0)	3.33	1.15	B
B2u	3.56 (348.16)	0.943	16% (3−0) + 46% (1−1) + 38% (0−0)	3.39 (365.67)	1.386	52% (1−0) + 45% (0−1)			
B3g	3.58 (346.41)	0.000	100% (2−0)	3.64 (340.55)	0.000	100% (2−0)	3.65	<0.1	N
Ag	3.79 (326.95)	0.000	100% (2−0)	3.87 (320.48)	0.000	100% (2−1)			
				FBC					
B2	2.28 (543.93)	0.098	32% (1−1) + 68% (0−0)	2.25 (550.47)	0.159	26% (1−1) + 74% (0−0)	1.98[c]	0.10	Qx
A1	2.52 (491.02)	0.001	54% (1−0) + 46% (0−1)	2.51 (493.63)	0.001	54% (1−0) + 46% (0−1)	2.29	0.06	Qy
A1	3.40 (364.18)	0.123	85% (2−0)	3.35 (370.08)	0.888	81% (1−1)			
B2	3.44 (359.97)	0.529	24% (2−1) + 63% (1−1)	3.36 (369.40)	1.276	37% (1−0) + 53% (0−1)	3.18	0.96	B
A1	3.64 (341.03)	1.069	27% (2−0) + 27% (1−0) + 46% (0−1)	3.61 (343.33)	0.221	97% (2−0)			
B2	3.93 (315.44)	0.330	89% (2−1) + 11% (1−1)	3.98 (311.24)	0.212	27% (5−0) + 73% (2−0)			
				FBBC					
B2u	2.10 (589.85)	0.243	77% (0−0) + 23% (1−1)	2.01 (617.81)	0.362	83% (0−0) + 17% (1−1)	1.6[d]	middle	Qx
B3u	2.57 (483.14)	0.048	64% (1−0) + 36% (0−1)	2.55 (486.29)	0.087	68% (1−0) + 32% (0−1)	2.3	middle	Qy
B3u	3.81 (325.83)	1.138	22% (1−0) + 78% (0−1)	3.61 (343.81)	1.362	19% (1−0) + 81% (0−1)	3.1	strong	By
B1g	3.98 (311.85)	0.000	23% (4−0) + 77% (2−0)	3.94 (314.40)	1.257	100% (1−1)			
B2u	4.10 (302.61)	1.112	96% (1−1) + 4% (0−0)	3.96 (313.06)	0.000	82% (2−0) + 18% (3−0)	3.4	strong	Bx
B3u	4.15 (299.15)	0.044	100% (3−0)	4.15 (298.69)	0.019	100% (4−0)			
				Pz					
B1u	2.42 (513.35)	0.157	27% (1−1) + 68% (0−0)	2.37 (523.60)	0.259	19% (1−1) + 75% (0−0)	2.01[e]		Qx
B2u	2.56 (484.05)	0.153	20% (1−0) + 72% (0−1)	2.50 (496.81)	0.267	12% (1−0) + 80% (0−1)	2.27		Qy
B1u	3.27 (379.65)	0.109	34% (3−1) + 60% (1−1)	3.21 (386.19)	0.145	22% (3−1) + 74% (1−1)	3.30		B
B3g	3.28 (377.38)	0.000	100% (2−0)	3.25 (381.41)	0.000	100% (2−0)			
B2u	3.38 (366.75)	0.048	39% (3−0) + 58% (1−0)	3.34 (371.03)	0.072	75% (1−0) + 25% (3−0)			
Ag	3.43 (361.94)	0.000	100% (2−0)	3.41 (363.52)	0.000	100% (4−0)			

[a] In parenthesis are reported the orbital contributions with the convention that the first number, n, refers to the occupied orbitals (HOMO-n), and the second (m) to the virtuals (LUMO + m) [b] gas phase, ref 43. [c] In benzene, ref 44. [d] Data for bacteriopheophorbide, ref 45. [e] In chlorobenzene, ref 51.

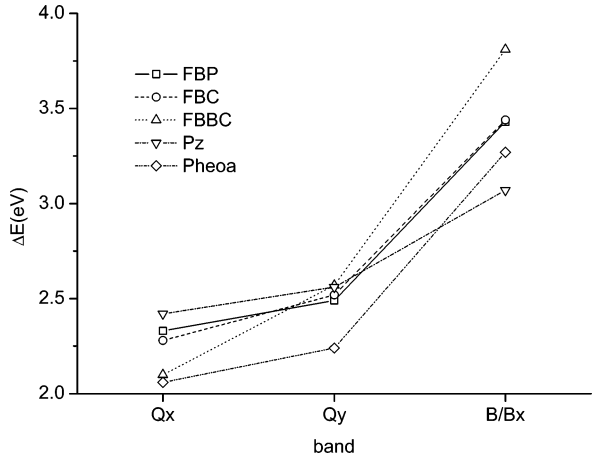

Figure 2. Plot of the transition energies (ΔE, eV) corresponding to the Q and Bx bands for some of the considered molecules.

Our results are also consistent with experimental values for B bands. For FBP and FBC, only one peak is observed, whereas the relaxation of degeneracy in FBBC gives rise to two bands (361 and 360 nm, respectively). The Bx band is markedly blue-shifted (303 nm) relative to the By one (326 nm), with high intensities in both cases (1.112 and 1.138, respectively) because the Bx band has a strong next-HOMO → next-LUMO character. For these two excitations, our work provides a better accuracy than previous SAC/SAC−CI calculations,[16] performed with a double-ζ Huzinaga's basis sets.

Porphyrazine (Pz) differs from free base porphyrin by the introduction of aza groups in the meso position (see Figure 1). As displayed in Figure 4, the orbital diagram is deeply affected with a significant stabilization of all frontier orbitals. In other words, the high amplitude of the meso nitrogens on the next-HOMO level (Figure 3) explains its strong stabilization (ΔE = 1.55 eV) with respect to FBP. This contribution remains high but is quite similar for LUMO and next-LUMO (ΔE_{LUMO} = 0.96 eV, $\Delta E_{\mathrm{next-LUMO}}$ = 0.86 eV), which are thus degenerate as for porphyrin. This stabilization is lower for the HOMO (ΔE = 0.62 eV). Despite this, the comparison with FBP transitions is not trivial because of an important interconfigurational mixing. As suggested by Parusel and Grimme,[17] all transitions involved in each band must be considered to rationalize the results. The Q bands shifts originate from a balance between the main configuration involved, whose energy is lowered in Pz with respect to FBP, and the second one that follows an opposite trend. Therefore, despite a large lowering of the HOMO/LUMO gap (ΔE = 0.34 eV), the Qx band is only displaced 0.07 eV downward. Likewise, a blue-shift of 0.23 eV is calculated for the Qy counterpart. Interpreting excitation values becomes even more difficult for B bands for which the Gouterman's model breaks down. The observed red-shift of 18 nm is indeed related to the minor HOMO-3 → LUMO + 1 transition. Experimental data support these qualitative interpretations and are quite close to our values. Even though the Qx band is overestimated of 0.4 eV, results get better when moving to the UV region. In particular, we found B band at 3.27 eV, that is 0.03 eV below

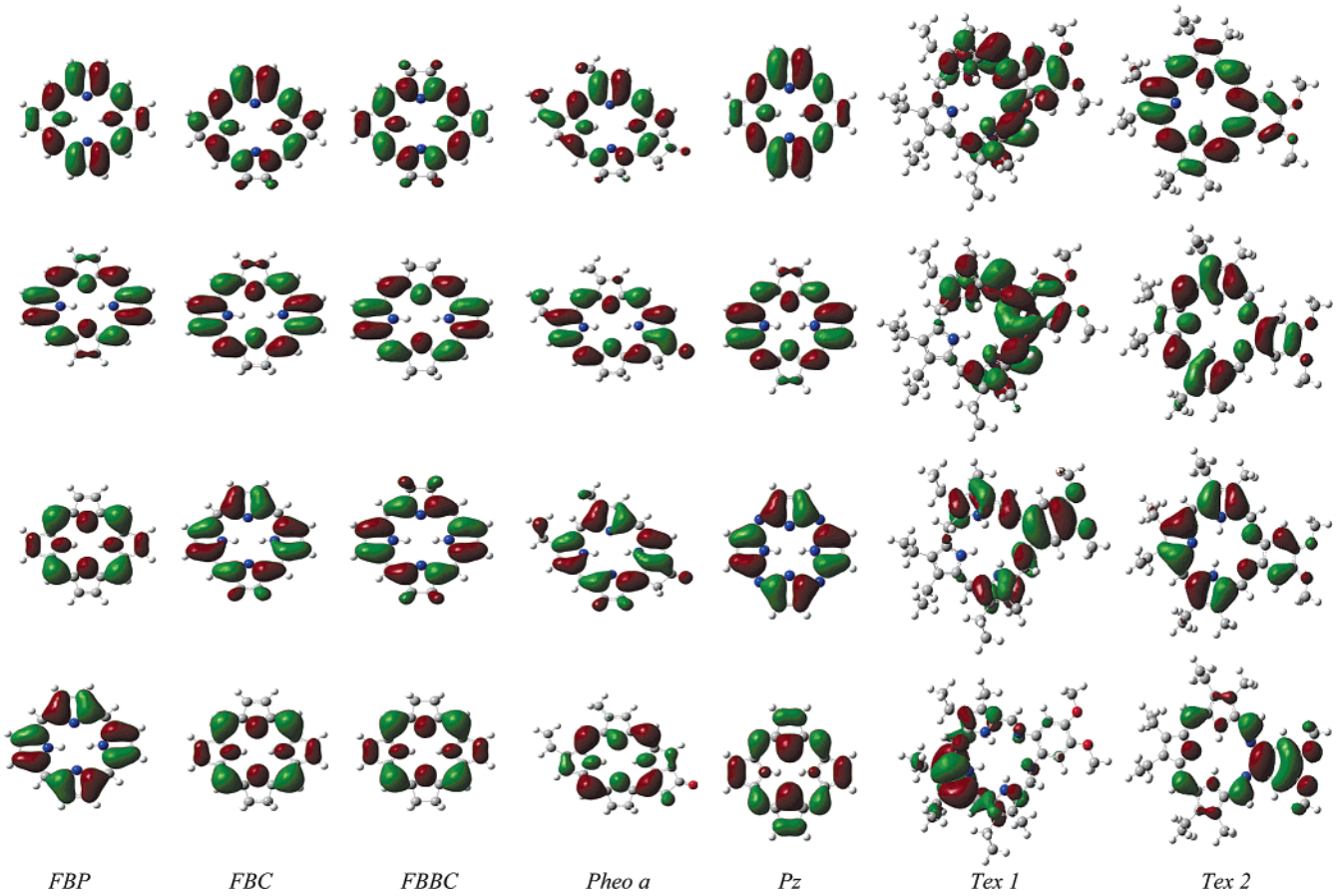

Figure 3. Illustration of the four Gouterman's orbitals for FBP, FBC, FBBC, Pheo a, Pz, Tex1, and Tex2. From top to bottom: next-LUMO, LUMO, HOMO, and next-HOMO.

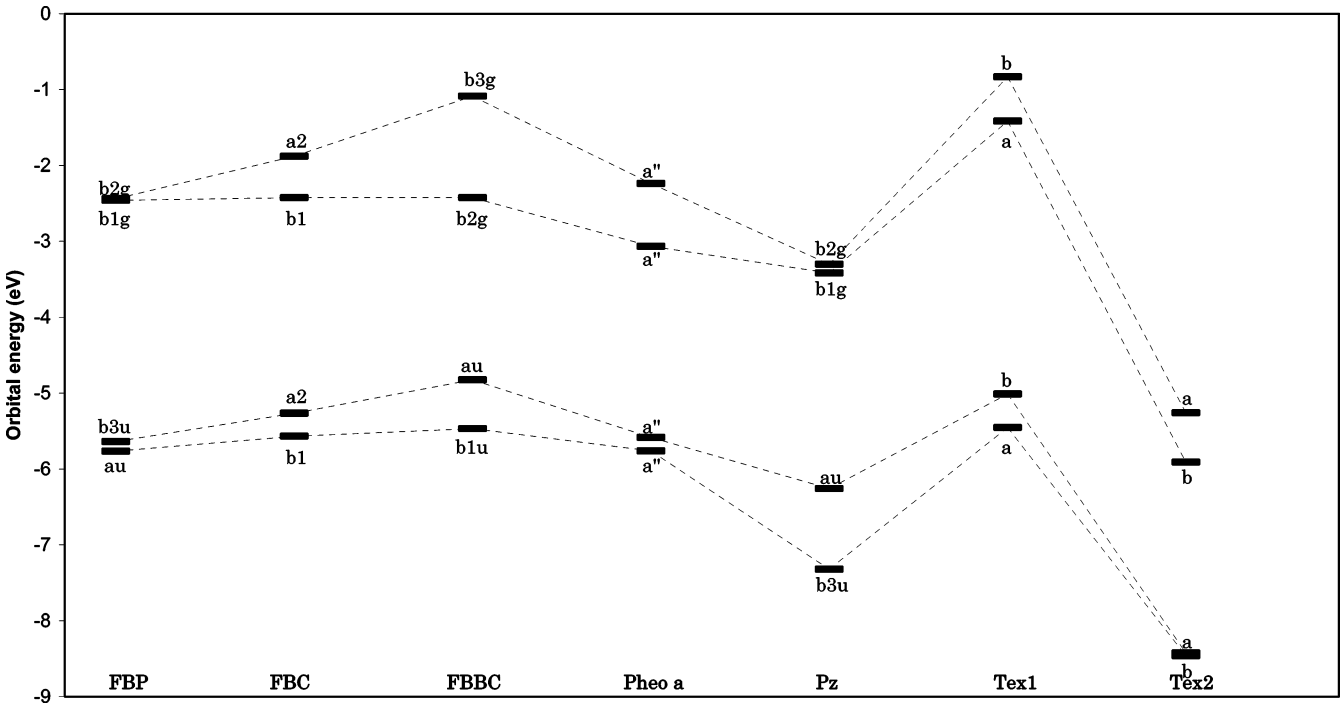

Figure 4. Evolution of the frontier orbitals energies for all the considered molecules.

the experimental counterpart, while SAC−CI and DFT/MRCI calculations give respective transitions at 3.56 and 2.97 eV.[16,17]

Actually, the noteworthy consequence of the introduction of aza groups is the appreciable intensification of Q bands, which explains why porphyrazines are industrially used as colorants. The more electronegative nitrogen atoms tend to concentrate the electronic density in the meso positions. The ring is thus polarized, and transition moments increase. As expected, the oscillator strengths in the visible part of the spectrum (Q bands) are found to be larger, with 0.157 and 0.153 for Qx and Qy

TABLE 2: Excitation Energies (eV and nm), Oscillator Strengths, Configurations, and Comparison with Experimental Data for Pheo a, Tex1, and Tex2[a]

	vacuum			solution (water PCM)			expt		
state	excitation energy, eV (nm)	oscillator strength	main configuration	excitation energy, eV (nm)	oscillator strength	main configuration	excitation energy, eV	oscillator strength	assignment
				Pheo a					
A′	2.06 (601.45)	0.211	73% (0−0) + 27% (1−1)	2.00 (618.82)	0.339	80% (0−0) + 20% (1−1)	1.9[b], 1.86[c], 1.87[d]		Qx
A′	2.24 (552.96)	0.048	72% (1−0) + 28% (0−1)	2.20 (562.38)	0.087	77% (1−0) + 23% (0−1)	2.3[b], 2.33[c], 2.30		Qy
A′	2.73 (454.04)	0.001	100% (2−0)	2.77 (448.05)	0.001	100% (2−0)			
A′	3.07 (404.19)	0.333	21% (2−1) +27% (1−1) + 39% (0−1)	2.99 (415.20)	0.498	69% (0−1) + 15% (1−1)	3.1[b], 3.04[c]		B
A′	3.22 (384.45)	0.550	22% (2−1) + 27% (1−1) + 36% (0−1)	3.12 (397.49)	0.969	55% (1−1) + 15% (0−1) + 12% (3−0)	3.2[c]		B
A″	3.25 (381.68)	0.000	93% (4−0)	3.18 (389.77)	0.043	88% (3−0)			
				Tex1					
B	2.85 (434.79)	0.232	100% (0−0)	2.89 (428.31)	0.303	100% (0−0)			
A	3.37 (367.66)	0.003	63% (1−0) + 37% (0−1)	3.39 (366.15)	0.023	89% (1−0) + 11% (0−1)			
A	3.47 (357.29)	0.270	14% (2−0) + 38% (1−0) + 48% (0−1)	3.49 (354.90)	0.392	79% (0−1) + 11% (1−0) + 10% (2−0)			
B	3.75 (330.76)	0.031	93% (3−0)	3.75 (331.06)	0.030	94% (3−0)			
A	3.87 (320.04)	0.793	90% (2−0)	3.81 (325.22)	0.934	95% (2−0)			
B	3.96 (312.68)	0.007	100% (1−1)	3.96 (312.83)	0.008	100% (1−1)			
A	4.32 (286.88)	0.079	18% (7−0) + 41% (5−0) + 15% (0−5) + 10% (3−1)	4.32 (286.80)	0.023	97% (2−1)			
B	4.33 (286.15)	0.022	92% (2−1) + 8% (4−0)	4.33 (286.42)	0.065	33% (5−0) + 26% (2−1) + 17% (7−0) + 15% (0−3)			
B	4.35 (284.97)	0.005	94% (4−0)	4.34 (285.38)	0.002	100% (4−0)			
B	4.43 (279.75)	0.009	79% (0−2) + 19% (0−4)	4.47 (277.47)	0.106	60% (3−1) + 29% (7−0)			
				Tex2					
B	1.98 (624.91)	0.066	71% (0−0) + 29% (1−1)	1.96 (633.64)	0.111	77% (0−0) + 23% (1−1)	1.73[e]		Qx
A	2.07 (598.65)	0.099	64% (1−0) + 36% (0−1)	2.05 (605.60)	0.181	69% (1−0) + 31% (0−1)			Qy
A	2.46 (505.05)	0.006	100% (2−0)	2.55 (486.61)	0.005	100% (2−0)			
B	2.85 (435.01)	0.130	54% (2−1) + 30% (1−1) + 11% (3−0)	2.85 (435.55)	0.371	57% (1−1) + 16% (2−1) + 18% (3−0)			
A	2.93 (422.95)	0.001	100% (6−0)	2.90 (428.17)	0.018	100% (6−0)			
B	3.04 (407.38)	0.093	45% (2−1) + 32% (3−0) + 14% (1−1)	2.93 (423.71)	1.769	74% (0−1) + 17% (1−0)			
A	3.07 (403.60)	1.310	55% (0−1) + 17% (1−0) + 17% (5−0)	3.08 (403.15)	0.012	90% (4−0) + 10% (2−1)	2.72[e]		B
B	3.14 (394.53)	0.005	88% (4−0) + 12% (3−0)	3.09 (400.72)	0.001	42% (2−1) + 35% (3−0) + 23% (4−0)			
A	3.17 (391.40)	0.273	89% (5−0)	3.10 (399.52)	0.096	100% (5−0)			
B	3.30 (373.31)	0.709	53% (3−0) + 25% (1−1)	3.21 (386.16)	0.804	53% (3−0) + 16% (2−1) + 20% (1−1)			

[a] In parenthesis are reported the orbital contributions with the convention that the first number, *n*, refers to the occupied orbitals (HOMO-*n*), and the second (*m*) to the virtuals (LUMO + *m*) [b] Reference 45. [c] In ether, ref 47. [d] In benzene, ref 48. [e] Reference 50.

bands, respectively. Moreover, in contrast with other tetrapyrroles, the intensity of Q bands in porphyrazines is higher than for the B ones ($f = 0.109$).

Pheophytin a (Pheo a) corresponds to the free base chlorophyll a. We remind the reader that a simplified form of Pheo a is considered herein. As reported by Hasegawa and co-workers,[16] its absorption spectrum is close to chlorine FBC because they only differ by substituent groups. Our calculations are in very good agreement with experimental data[44,47−48] for both Q and B bands. We find respective discrepancies of 0.07 eV for the Qx band, 0.06 eV for the Qy band, and around 0.03 eV for the B ones (Table 2). In comparison with previous SAC/SAC−CI results,[16] a similar accuracy is found for Q bands, while B bands are better described in our study. On the whole, both Q and B bands are displaced to higher wavelengths relative to FBC, up to 62 nm for the Qy transition, and indeed, Figure 4 points out that Pheo a frontier orbitals are stabilized, the introduction of a vinyl group and a carbonyl function strengthening the conjugation of the whole porphyrin ring. The greatest stabilization is observed for the LUMO ($\Delta E = 0.64$ eV), where there is a great contribution of both new substituents (see Figure 3). On the contrary, they do not participate in the next-HOMO level, whose stabilization is therefore the lowest ($\Delta E = 0.19$ eV). Gouterman's orbitals are hence unevenly stabilized. Energy differences between these levels are lower than for FBC, resulting in a global red-shift. Oscillator strengths are also deeply intensified for Q bands ($f_{Qx} = 0.211$; $f_{Qy} = 0.048$) because the substitution breaks down the symmetry. Transition moment components are thereby totally modified.

Experimentally, free base texaphyrin has been synthesized in two forms (Figure 1)**.** The first one, referred to herein as Tex1, is used when preparing metallotexaphyrins and is characterized by sp^3 carbons in the meso position.[49] Tex2 is the aromatic form of texaphyrin:[50] it is positively charged and is found as a salt in solid or liquid (acetonitrile, benzonitrile) states. Calculations were performed on these two forms of texaphyrins so as to compare the effect of conjugation on excited states. Indeed, from a geometrical point of view, Tex1 could assume twisted conformations, whereas Tex2 should remain locally planar. That is why the C_2 symmetry was imposed while optimizing Tex2. In contrast, we obviously found Tex1 to be the most stable when relaxing the geometry. Because the main

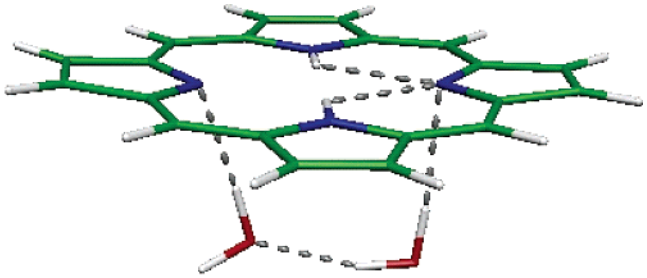

FBP with 2 water molecules

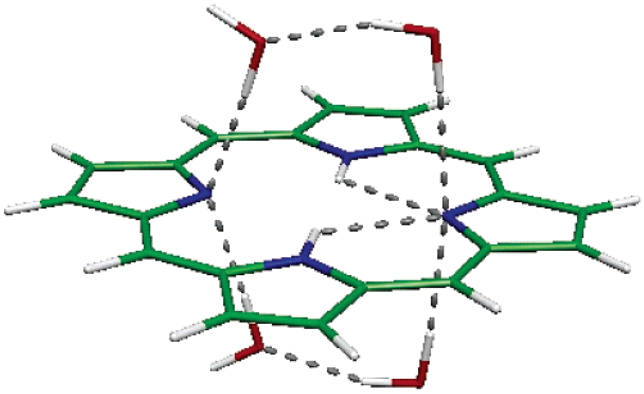

FBP with 4 water molecules

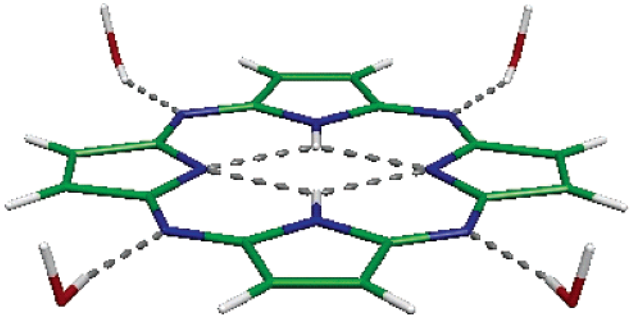

Pz with 4 water molecules

Figure 5. Structures of the free base porphyrin and free base porphyrazine with 2 and 4 explicit water molecules.

ring is not conjugated, frontier orbitals are markedly destabilized, as shown in Figure 4. The Q bands are, therefore, found to be very low in energy, respectively at 2.85 and 3.37 eV, as is their B counterpart (3.87 eV).

Because the ultimate goal of our study is to understand properties of molecules involved in photodynamic therapy, Tex2 seems thus much more interesting thanks to the aromatic ring. As expected, all levels are significantly stabilized with respect to Tex1, and more generally with respect to all other systems studied herein. This is not surprising when one knows that metalated texaphyrins are already used in clinical tests.[5,6] On the whole, our results are consistent with experimental values,[50] the mean absolute error being about 12% (Table 2). Tex2 exhibits Qx and Qy bands at 1.98 and 2.07 eV, respectively, whereas the experimental counterpart is observed at 1.73 eV.

3.2. Excited States in Water: Solvation Effects. Using photosensitizers in PDT is quite challenging, notably because the biological environment can modify or even alter their spectral properties. In this regard, the behavior in aqueous solution must be considered. Solvent (water) effects can be theoretically evaluated in two ways. The most straightforward approach is to add explicit water molecules, corresponding to the first solvation shell. One can indeed foresee that pyrrole nitrogens should form hydrogen bonds with water. We have thus used either 2 or 4 water molecules in interaction with FBP, FBBC, and Pz. Some of the optimized geometries are depicted in Figure 5. On the whole, even if the system slightly tends to lose its planar conformation, geometrical changes remain negligible. Q and B bands are logically almost unaffected, with $Qx_{(FBP-4H2O)} = 532$ nm ($Qx_{(FBP)} = 524$ nm) or $B_{(Pz-4H2O)} = 380$ nm ($B_{(Pz)} = 386$ nm) for instance. It is in contrast worth noting that the spectral region below can exhibit some charge-transfer transitions between oxygen p orbitals of the solvent molecules and π^* levels of the ligand. They are often mixed with $\pi-\pi^*$ transitions, as in tetrahydrated porphyrin, where intense bands are calculated at 340 nm ($f = 0.27$), 333 nm ($f = 0.15$), or 329 nm ($f = 0.26$).

Solvation effects can also be considered by using a continuum model. The reaction field generated by the interaction with the bulk solvent can greatly modulate the electronic distribution of the solute, thereby affecting its spectral properties.[30] Excitation energies, oscillator strengths, and assignments calculated on the seven systems with the C-PCM model are summarized in Tables 1 and 2. The effect of bulk solvent is globally quite low, as expected in the case of $\pi-\pi^*$ transitions. In fact, energy levels and Gouterman's orbitals' shape do not significantly change in the presence of the solvent reaction field. Concerning spectral properties, both Qx and B bands are shifted upward, up to 28 nm for FBBC, while Qy bands are not affected. As one can expect, the red-shift is especially significant for systems with an important symmetry breakdown (FBBC, Pheo a) or for charged systems (Tex2). The reaction field then strongly stabilizes orbitals and makes transition moments higher, thus accounting for the strengthening of the computed excitations. For instance, the increase in oscillator strengths can reach 0.5 units for B bands.

Looking upon spectral properties, Tex2, Pheo a, and FBBC turn out to be the best candidates for applications in photodynamic therapy, as already found experimentally.[4] They are all the more interesting given that this trend is strengthened when being in aqueous phase.

4. Conclusion

The calculation of the excited states of seven porphine derivatives with a high biological interest, namely porphyrin, chlorin, bacteriochlorin, porphyrazine, pheophytin a, and two different texaphyrins, was carried out. Each complex was carefully studied and compared to the others by analyzing both energetic and orbital aspects within a DFT approach. The electronic spectra, calculated by using the TDDFT route, are in good agreement with experimental data. In the perspective of therapeutic applications, the behavior in aqueous phase was worked out. Whereas the supramolecular approach does not affect results, the C-PCM continuum model shifts Qx and B bands upward, reducing discrepancies with experimental data. The polarization is also improved and greatly strengthens band intensities.

Tex2, Pheo a, and FBBC are found to be the most interesting molecules for potential applications in photodynamic therapy. These results are particularly encouraging for future theoretical studies on metalated complexes as well as for guiding experimentalists' works.

Acknowledgment. Financial support from the Università degli Studi della Calabria and Regione Calabria (POR Calabria 2000/2006, misura 3.16, progetto PROSICA) is gratefully

acknowledged. C.A. and L.P. are grateful to the French National Computer Center (IDRIS) for a generous grant of computer time (project 41703). L.P. also wishes to thank Università della Calabria for a grant and the kind hospitality shown to her while a visitor.

References and Notes

(1) MacDonald, I. J.; Dougherty, T. J. *J. Porphyrins Phthalocyanines* **2001**, *5*, 105.
(2) Sono, M.; Roach, M. R.; Coulter, E. D.; Dawson, J. H. *Chem. Rev.* **1996**, *96*, 2841.
(3) Kadish, K. M.; Smith, K. M.; Guilard, R. *The Porphyrin Handbook*; Academic: New York, 1978.
(4) Detty, M. R.; Gibson, S. L.; Wagner, S. J. *J. Med. Chem.* **2004**, *47*, 3897.
(5) Rosenthal, D. I.; Nurenberg, P.; Becerra, C. R.; Frenkel, E. P.; Carbone, D. P.; Lum, B. L.; Miller, R.; Engel, J.; Young, S.; Miles, D.; Renschler, M. F.; *Clin. Cancer Res.* **1945**, *5*, 739.
(6) Rockson, S. G.; Kramer, P.; Razavi, M.; Szuba, A.; Filardo, S.; Adelman, D. C. *Circulation* **2000**, *102*, 2322.
(7) Sundholm, D. *Phys. Chem. Chem. Phys.* **2000**, *2*, 2275.
(8) Ghosh, A. *J. Phys. Chem. B* **1997**, *101*, 3290.
(9) Miwa, H.; Makarova, E. A.; Ishii, K.; Luk′yanets, E. A.; Kobayashi, N. *Chem.—Eur. J.* **2002**, *8*, 1082.
(10) Parusel, A. B. J.; Ghosh, A. *J. Phys. Chem. A* **2000**, *104*, 2504.
(11) Oliveira, K. M. T.; Trsic, M. *J. Mol. Struct.* **2001**, *539*, 107.
(12) Yamaguchi, Y.; Yokoyama, S.; Mashiko, S. *J. Chem. Phys.* **2002**, *116*, 6541.
(13) Seda, J.; Burda, J. V.; Leszczynski, J. *J. Comput. Chem.* **2004**, *26*, 294.
(14) Linnanto, J.; Korppi-Tommola, J. *J. Phys. Chem. A* **2001**, *105*, 3855.
(15) Hashimoto, T.; Choe, Y.-K.; Nakano, H.; Hirao, K. *J. Phys. Chem. A* **1999**, *103*, 1894.
(16) Hasegawa, J.; Ozeki, Y.; Ohkawa, K.; Hada, M.; Nakatsuji, H. *J. Phys. Chem. B* **1998**, *102*, 1320.
(17) Parusel, A. B. J.; Grimme, S. *J. Porphyrins Phthalocyanines* **2001**, *5*, 225.
(18) Baerends, E. J.; Ricciardi, G.; Rosa, A.; Van Gisbergen,S. J. A. *Coord. Chem. Rev.* **2002**, *230*, 5.
(19) Kuzmitsky, V. A.; Makarova, E. A.; Pershukevich, P. P.; Shushkevich, I. K.; Solovyov, K. N.; Tusov, V. B. *Chem. Phys.* **2004**, *298*, 1.
(20) Petit, L.; Adamo, C.; Russo, N. *J. Phys. Chem B* **2005**, *109*, 12214.
(21) Kuhn, H. *J. Chem. Phys.* **1949**, *17*, 1198.
(22) Simpson, W. T. *J. Chem. Phys.* **1949**, *17*, 1218.
(23) Almlof, J. *Int. J. Quantum Chem.* **1974**, *8*, 915.
(24) Momicchioli, F.; Baraldi, I.; Bruni, M. C. *Inorg. Chim. Acta*. **1983**, *82*, 229.
(25) Baker, J. D.; Zerner, M. C. *Chem. Phys. Lett.* **1990**, *175*, 192.
(26) Parac, M.; Grimme, S. *J. Phys. Chem. A* **2002**, *106*, 6844.
(27) Liao, M.-S.; Scheiner, S. *J. Chem. Phys.* **2002**, *117*, 205.
(28) Gross, E. U.K.; Dobson, J. F.; Petersilka, M. In *Density Functional Theory II*; Nalewajski, R. F., Ed.; Springer: Heidelberg, 1996.
(29) Adamo, C.; Scuseria, G. E.; Barone, V. *J. Chem. Phys.* **1999**, *111*, 2889.
(30) Adamo, C.; Barone, V. *Chem. Phys. Lett.* **2000**, *330*, 152.
(31) Guillemoles, J. F.; Barone, V.; Joubert, L.; Adamo, C. *J. Phys. Chem. A* **2002**, *106*, 11354.
(32) Frisch, M. J.; Trucks, G. W.; Schlegel, H. B.; Scuseria, G. E.; Robb, M. A.; Cheeseman, J. R.; Montgomery, J. A., Jr.; Vreven, T.; Kudin, K. N.; Burant, J. C.; Millam, J. M.; Iyengar, S. S.; Tomasi, J.; Barone, V.; Mennucci, B.; Cossi, M.; Scalmani, G.; Rega, N.; Petersson, G. A.; Nakatsuji, H.; Hada, M.; Ehara, M.; Toyota, K.; Fukuda, R.; Hasegawa, J.; Ishida, M.; Nakajima, T.; Honda, Y.; Kitao, O.; Nakai, H.; Klene, M.; Li, X.; Knox, J. E.; Hratchian, H. P.; Cross, J. B.; Bakken, V.; Adamo, C.; Jaramillo, J.; Gomperts, R.; Stratmann, R. E.; Yazyev, O.; Austin, A. J.; Cammi, R.; Pomelli, C.; Ochterski, J. W.; Ayala, P. Y.; Morokuma, K.; Voth, G. A.; Salvador, P.; Dannenberg, J. J.; Zakrzewski, V. G.; Dapprich, S.; Daniels, A. D.; Strain, M. C.; Farkas, O.; Malick, D. K.; Rabuck, A. D.; Raghavachari, K.; Foresman, J. B.; Ortiz, J. V.; Cui, Q.; Baboul, A. G.; Clifford, S.; Cioslowski, J.; Stefanov, B. B.; Liu, G.; Liashenko, A.; Piskorz, P.; Komaromi, I.; Martin, R. L.; Fox, D. J.; Keith, T.; Al-Laham, M. A.; Peng, C. Y.; Nanayakkara, A.; Challacombe, M.; Gill, P. M. W.; Johnson, B.; Chen, W.; Wong, M. W.; Gonzalez, C.; Pople, J. A. *Gaussian 03*, revision B.05; Gaussian, Inc.: Wallingford, CT, 2004.
(33) Adamo, C.; Barone, V. *J. Chem. Phys.* **1999**, *110*, 6158.
(34) Perdew, J. P.; Burke, K.; Ernzerhof, M. *Phys. Rev. Lett.* **1996**, *77*, 3865; **1997**, *78*, 1396.
(35) Francl, M. M.; Petro, W. J.; Hehre, W. J.; Binkley, J. S.; Gordon, M. S.; DeFrees, D. J.; Pople, J. A. *J. Chem. Phys.* **1982**, *77*, 3654.
(36) Hasegawa, J.; Ozeki, Y.; Ohkawa, K.; Hada, M.; Nakatsuji, H. *J. Phys. Chem. B* **1998**, *102*, 1320.
(37) Stratmann, R. E.; Scuseria, G. E.; Frisch, M. J. *J. Chem. Phys.* **1998**, *109*, 8128.
(38) Tomasi, J.; Persico, M. *Chem. Rev.* **1994**, *94*, 2027.
(39) Barone, V.; Cossi, M. *J. Phys. Chem. A* **1998**, *102*, 1995.
(40) Cossi, M.; Barone, V. *J. Chem. Phys.* **2001**, *115*, 4708.
(41) Gouterman, M.; Wagniere, G. H.; Snyder, L. C. *J. Mol. Spectrosc.* **1963**, *11*, 108.
(42) Edwards, L.; Dolphin, D. H. *J. Mol. Spectrosc.* **1971**, *38*, 16.
(43) Nagashima, U.; Takada, T.; Ohno, K. *J. Phys. Chem.* **1986**, *85*, 4524.
(44) Scheer, H.; Inhoffen, H. H. In *The Porphyrins*; Dolphin, D., Ed.; Academic Press: New York, 1978; Vol. II, pp 45—90.
(45) Dreuw, A.; Head-Gordon, M. *J. Am. Chem. Soc.* **2004**, *126*, 4007.
(46) Weiss, C. In *The Porphyrins*; Dolphin, D., Ed.; Academic Press: New York, 1978; Vol. III, Part A, Physical Chemistry.
(47) Houssier, C.; Sauer, K. *J. Am. Chem. Soc.* **1970**, *92*, 779.
(48) Eisner, U.; Linstead, R. P. *J. Chem. Soc.* **1955**, 3742.
(49) Hannah, S.; Lynch, V.; Guldi, D. M.; Gerasimchuk, N.; MacDonald, C. L. B.; Magda, D.; Sessler, J. L. *J. Am. Chem. Soc.* **2002**, *124*, 8416.
(50) Hannah, S.; Lynch, V.; Guldi, D. M.; Gerasimchuk, N.; MacDonald, C. L. B.; Magda, D.; Sessler, J. L. *Org. Lett.* **2001**, *3*, 3911.
(51) Linstead, R. P.; Whally, M. *J. Chem. Soc.* **1952**, 4839.